Vol. 15, No. 5 (2026): 1646 - 1657 http://dx.doi.org/10.23960/jtepl.v15i5.1646-1657

JURNAL TEKNIK PERTANIAN LAMPUNG

ISSN 2302-559X (print) / 2549-0818 (online)
Journal homepage : https://jurnal.fp.unila.ac.id/index.php/JTP

Determination of Modified Atmosphere Critical Limits to Minimize Postharvest Decay and Quality Loss in Red Chili Pepper

Halimatus Sa'diya[1], Muhammad Alfian[1], Yoga Arif Firmansyah[1], Sri Rahayoe[1], Bayu Nugraha[1,✉]

[1] Department of Agricultural and Biosystem Engineering, Faculty of Agricultural Technology, Universitas Gadjah Mada, Yogyakarta, INDONESIA.

Article History:

Received : 30 January 2026
Revised : 08 August 2026
Accepted : 25 August 2026

Keywords:

Chili pepper,
Critical oxygen level,
Michaelis-Menten,
X-ray CT.

Corresponding Author:
✉ bayu.nugraha@ugm.ac.id
(Bayu Nugraha)

ABSTRACT

Respiratory responses of individual chili pepper based on anatomical structures are remain poorly understood. Characterizing these responses is essential for determining the critical oxygen level (COL) and understanding tissue-specific O_2 limitations under modified atmospheres. This study quantified O_2 consumption and CO_2 production in intact fruits and individual anatomical structures using a gas analyser and integrated respiration modelling with X-ray computed tomography (CT) to characterize internal pathways for gas transport. Intact fruits and pericarp showed a rapid decrease in O_2 concentration, whereas seeds and pedicels exhibited slower O_2 declines without complete depletion. Michaelis–Menten modelling revealed anatomical structure- and maturity-dependent differences in COL. The COL of intact fruits decreased from 0.44% O_2 at the green stage to 0.12% at the orange stage and 0.08% at the red stage, whereas the pedicel showed substantially higher COL values (2.13–11.51% O_2) than the seed (0.17–1.80% O_2) and pericarp (0.02–0.07% O_2). X-ray CT revealed internal air spaces connected to the pedicel, providing structural evidence of a potential pathway for O_2 transport towards internal tissues. By integrating COL of individual anatomical structures with three-dimensional internal architecture, this study extends conventional intact chili respiration approaches and provides a physiological basis for defining modified-atmosphere conditions that minimize localized O_2 limitation in chili pepper.

1. INTRODUCTION

Chili pepper (*Capsicum annuum)* is an economically and nutritionally vital commodity in Indonesia, but its highly perishable nature consistently causes post-harvest quality degradation and market instability (Surya & Tedjakusuma, 2022; Lestari *et al*., 2022). The post-harvest quality of chili pepper is related to its perishable nature. This quality is influenced by several factors, including physiological damage during handling, packaging, storage, and transportation (Mahajan *et al*., 2017; Munarso *et al*., 2020). Physiological damage will trigger a high respiration rate, as indicated by the rate of O_2 consumption and CO_2 production (Pathare *et al*., 2023). High respiration rates can be overcome by reducing O_2 and increasing CO_2, but there is the potential for fermentation processes to occur, which produce ethanol and accelerate physiological damage to the fruit (Brizzolara *et al*., 2020). In addition, post-harvest ripeness and temperature are factors that influence respiration activity. Respiration rates in Capsicum cultivars vary; some increase with maturation, while others decrease (Del Giúdice *et al*., 2023).

Moreover, respiration rates vary among fruit organs, such as seeds and pedicels (Xiao *et al*., 2018), reflecting differences in gas exchange within the heterogeneous structure of horticultural products (Nugraha *et al*., 2022). Despite these differences, respiration in chili pepper has largely been evaluated at the intact chili ((Chitravathi *et al*., 2015; Malakar *et al*., 2020), leaving the respiratory responses and critical O_2 levels of individual internal structures unresolved.

© 2026 The Authors
This work is licensed under a Creative Commons Attribution-ShareAlike 4.0 International License.

Respiration measurements typically use a closed system. Short-term measurements typically use a closed system method, which assumes a linear change over time (Ho *et al*., 2020). The advantage of closed-system respiration measurements is that they allow testing various gas combinations with simple equipment and are suitable for products with low respiration rates. However, changes in O_2 and CO_2 are inversely correlated, which necessitates a practical, integral method for analyzing respiration rates using a respiration model (Ho *et al*., 2020). Because respiration is mainly an enzyme-catalyzed process, the rate saturates at high O_2 rather than increasing linearly, so that models of respiration are based on enzyme kinetics (Castellanos *et al*., 2017).

The complexity of the respiratory pathway in horticultural products is often simplified to a single rate-limiting enzymatic reaction, commonly described by a Michaelis–Menten model expressed as a function of gas composition. CO_2 inhibition is incorporated through competitive, uncompetitive, noncompetitive, or mixed forms, which differ in where CO_2 binds relative to the substrate (Castellanos *et al*., 2017). This model has been applied to a range of horticultural products (Garavito *et al*., 2021; Castellanos *et al*., 2017). In the present study, the non-competitive inhibition model was adopted because the uncompetitive model of inhibition fitted best with the experimental results.

Interpreting respiration at the level of individual fruit parts, however, requires knowing how those parts are arranged within the fruit and how much of its volume each occupies. Conventional dissection provides this information only destructively, one fruit at a time, and cannot preserve the spatial relationships between tissues. X-ray computed tomography (CT) resolves internal structure non-destructively from differences in tissue density, and has been applied to characterize the internal architecture of a range of horticultural products (Du *et al*., 2019). In the present study, X-ray CT was used to visualize the seeds, placenta, pericarp, and pedicel in three dimensions, providing the structural context in which the measured respiration of each anatomical part could be interpreted. The aim of this study was therefore to determine the respiration characteristics and critical O_2 levels of individual anatomical parts of chili pepper across maturity stages, and to relate these to the internal structure resolved by X-ray CT, providing a basis for the design of storage and packaging systems.

2. MATERIALS AND METHODS

2.1. Sample preparation

Chili peppers were obtained from farmers in Pucanganom Village, Srumbung District, Magelang Regency, Central Java, Indonesia, during the harvest seasons of January and July 2025. Chili peppers were harvested from the same orchard and transported to the laboratory within approximately one hour to minimize post-harvest physiological changes. Upon arrival, the chili peppers were immediately washed with water, dried gently using tissue paper, and visually sorted to remove any fruits with skin damage. Only fruits with homogeneous size and color were selected for this study. The selected chili peppers were then classified according to their ripeness levels, namely large green (LG), initial coloring, and full red, referring to Hou *et al*. (2018). Representative samples of the chili peppers at these three maturity stages are shown in Figure 1.



Figure 1. Chili pepper samples with ripeness levels (A) LG: Large Green, (B) IC: Initial Coloring, and (C) FR: Full Red

2.2. Experimental setup

This study employed a randomized factorial design involving two main factors, namely chili pepper anatomy and maturity levels. The anatomical factor was divided into five categories, consisting of intact chili pepper, intact chili pepper without pedicel, pericarp, seeds, and pedicel. Meanwhile, the maturity level factor was grouped into three physiological phases: LG, IC, and FR as previously mentioned. The combination of these two factors resulted in 15 treatment groups, with each group consisting of 10 replications.

Prior to respiration analysis, the samples were separated into their respective anatomical parts. The physical properties of each category were then quantified. The mass of each sample was individually weighed, and the volume was measured using a standard water displacement method. As a baseline, the average weights of intact chili peppers, intact chili peppers without pedicel, pericarp, seed, and pedicels across the ripening stages were 1.81 g, 1.70 g, 1.34 g, 0.36 g, and 0.11 g, respectively. The corresponding average volumes were 2.56 mL, 1.85 mL, 1.28 mL, 0.60 mL, and 0.68 mL.

2.3. Critical oxygen limit

The respiration rate of red chili pepper was first measured in tightly closed 30 mL glass vials, equipped with a rubber septum for gas sampling (Figure 2). Fruit with and without pedicels, at each of the three maturity stages: large green (LG), initial coloring (IC), and full red (FR), were assessed individually, with five replicate vials per fruit condition combination (n = 10).

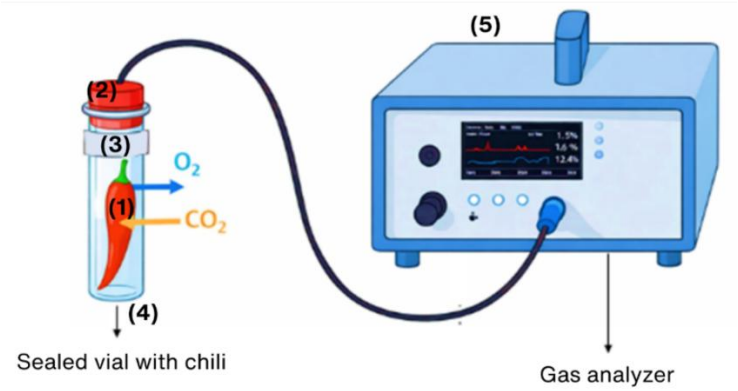


Figure 2. Airtight close respirometer chamber for analysis of respiration data set of chili pepper, where (1) a sample of chili pepper, (2) rubber septum, (3) head space, (4) close chamber, and (5) gas analyzer

Changes in headspace O_2 and CO_2 concentrations were monitored using a benchtop O_2/CO_2 headspace analyzer (Model 902D O_2/CO_2; Quantek Instruments, Inc., Grafton, MA, USA). O_2 consumption and CO_2 production rates were calculated according to Eq.(1) and (2):

$$R_{O_2} = \frac{\Delta C_{O_2}}{100 \cdot \Delta t} \cdot \frac{V}{m} \quad (1)$$

$$R_{CO_2} = \frac{\Delta C_{CO_2}}{100.\Delta t} \cdot \frac{V}{m} \quad (2)$$

where R_{O_2} and R_{CO_2} (mL.kg^{-1}.h^{-1}) are O_2 consumption and CO_2 production, respectively; ΔC_{O_2} and ΔC_{CO_2} (%) are the concentration difference of O_2 and CO_2, respectively, at initial and subsequent measurement times; Δt (h) is the measurement time; m (kg) is the sample weight; V (mL) is the headspace or free volume of the vial.

A non-competitive inhibition model (Eq. 3) was employed to characterize O_2 consumption during respiration (Triardianto *et al*., 2026). This model was selected because CO_2 acts as a non-competitive inhibitor in horticultural

produce, where elevated CO_2 levels inhibit O_2 consumption regardless of the ambient oxygen concentration. This provides an accurate representation of the enzymatic mechanics governing chili peppers' respiration under a modified atmosphere.

$$R_{O_2} = -\frac{V_{m,O_2} \cdot C_{O_2}}{\left(K_{m,O_2} + C_{O_2}\right) \cdot \left(1 + \frac{C_{CO_2}}{K_{mn,CO_2}}\right)} \tag{3}$$

where K_{m,O_2} (%) is the Michaelis-Menten constant for O_2 consumption, K_{mn,CO_2} (%) is the Michaelis-Menten constant for non-competitive CO_2 inhibition, and V_{m,O_2} (mL.g^{-1}.h^{-1}) is the maximum oxygen consumption rate.

Based on a modified version of the model by (Triardianto *et al*., 2026), the total CO_2 production rate (R_{CO_2}) was modelled as the sum of oxidative and fermentative contribution (Eq.4):

$$R_{CO_2} = -rq_{ox} \cdot R_{O_2} + \frac{V_{m,CO_2}}{\left(1 + \frac{C_{O_2}}{K_{mn,f,O_2}}\right)} \tag{4}$$

where rq_{ox} is respiratory quotient of oxidative respirations, K_{mn,f,O_2} (%) is the Michaelis constant for the suppression of fermentative CO_2 production by O_2, and V_{m,CO_2} (mL.kg^{-1}.h^{-1}) is the maximum fermentative CO_2 production rate.

Subsequently, the critical oxygen limit was calculated from the respiratory data according to Eq. 5, adopted from Nugraha *et al*. (2022).

$$C^*_{O_2} = \frac{f_f \cdot V_{mn,f,CO_2} \cdot K_{m,O_2}}{f_0 \cdot V_{m,O_2} \cdot rq_{ox} - f_f \cdot V_{mn,f,CO_2}} \tag{5}$$

where f_0 and f_f values represent the rates of oxygen consumption via oxidative respiration and carbon dioxide production via fermentation, respectively, as reported by Nugraha *et al*. (2022).

2.4. Critical respiratory quotient

The external RQ value is generally used in Eq. (6). In this study, the respiratory quotient (RQ) limit was calculated from external measurements of O_2 and CO_2 concentrations, as shown below, where all symbols are as defined in Section 2.3.

$$RQox = \frac{VCO_2 - \left(\frac{VmCO_2(f)}{1 + \frac{O_2}{KmO_2(f)}}\right)}{VO_2} \tag{6}$$

2.5. Three-dimensional Image Visualization

The 3D visualization of chili peppers was conducted using an X-ray CT system (V|tome|x S). A total of 30 representative samples from each maturity level were scanned. A macroscale resolution of 84.55 µm was selected to optimize the field of view (FOV) required to encompass the intact fruit geometry while providing sufficient spatial resolution to distinguish internal macro-structural features and air spaces. To ensure the clarity of the image, ImageJ (1.54g, National Institute of Health, USA) was considered by determining the dynamic range. The clearer image continued the segmentation process, which was conducted using open-source software, 3D Slicer (5.8.0, The Slicer Community, Brigham and Women's Hospital, USA), to reveal the respiration path of the chili pepper. The Otsu thresholding was applied to make a 3D macro-geometry of the chili pepper; the algorithm of growing from seeds was used to characterize the respiration path based on the placenta.

2.6. Data and Statistical Analysis

The kinetic parameters of the Michaelis-Menten respiration models were estimated using nonlinear regression (Solver tool) by minimizing the sum of squared residuals between the observed and predicted gas data (Han *et al*., 2020). The model was validated using the coefficient of determination (R^2) and Root Mean Square Error (RMSE). To evaluate the effects of chili pepper anatomy and maturity levels, experimental data were analyzed using a one-way ANOVA. Significant differences between treatment means ($p < 0.05$) were separated using Duncan's test via SPSS software.

3. RESULTS AND DISCUSSION

3.1. Oxygen and carbon dioxide profiles of the chili pepper anatomical parts

The experimental results showed the profiles of gas composition inside the containers with chili peppers at different anatomical parts and levels of ripeness (Figure 3). The results were as expected, showing a consistent trend throughout the analysed period, with a decrease in oxygen and an increase in CO_2 across all treatments. Figure 3 also shows that oxygen consumption occurs more rapidly at the large green of the ripening stage (Figure A1-A3; B1-B3; C1-C3; D1-D3; E1), which is marked by a concentration of 0% at 252 hours. Measurements in the large green stage were stopped before the oxygen concentration does not reach 0% because the concentration stagnated and has been contaminated by mold due to the rapid spoilage and cell lysis (Benkeblia, 2021). However, intact chili pepper, intact chili pepper without pedicel, and pericarp of the anatomical part were measured until O_2 concentration reached 0%, a process that required 312 hours for initial colouring and full red of the maturation stage (Fig. A2-E2 and A3-E3). The same phenomenon occurs during the initial coloration and full red stages, although the incubation period is longer.

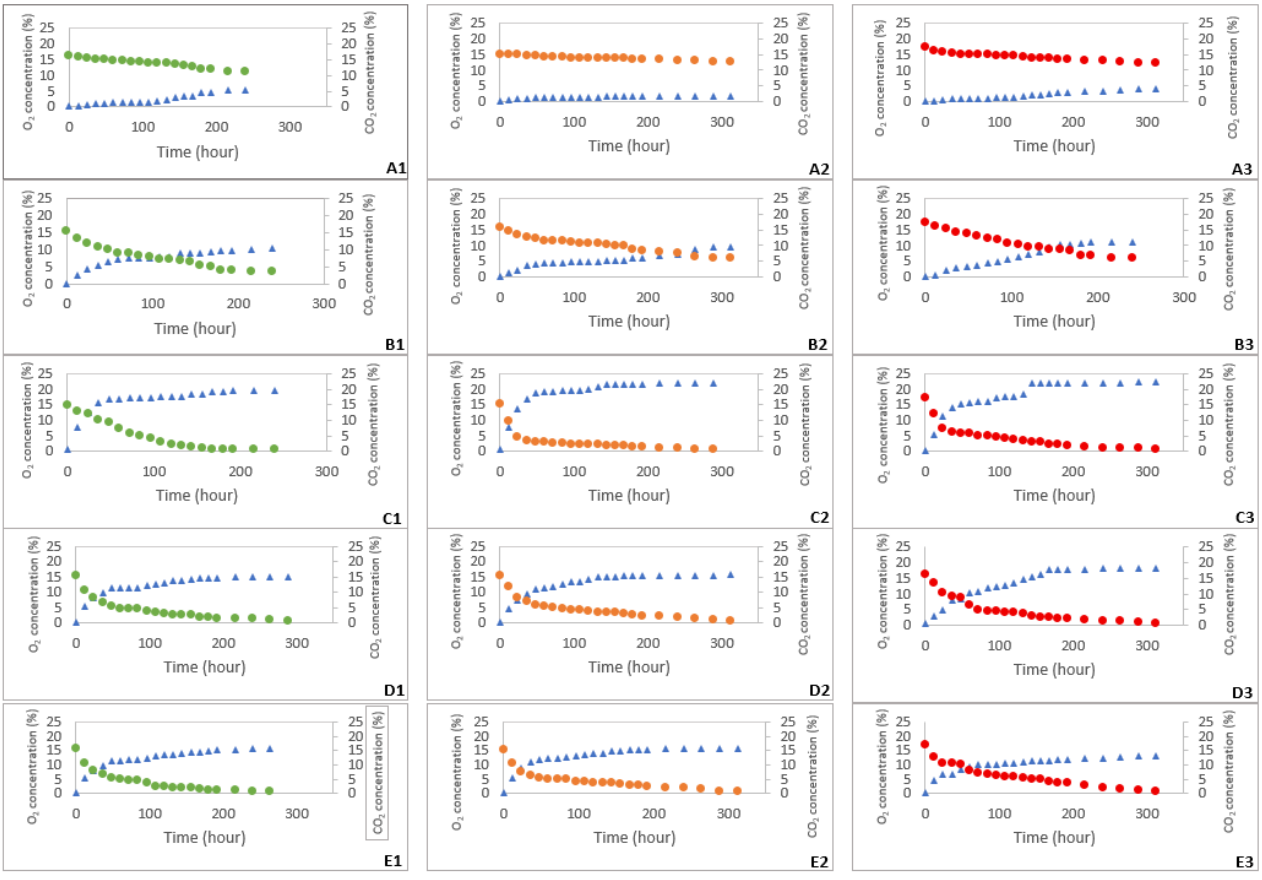


Figure 3. Changes in O2 (●) and CO_2 (▲) concentrations over time for different anatomical parts and maturity stages of chili peppers. The panel represents (A) pedicel, (B) seeds, (C) pericarp, (D) intact chili pepper without pedicel, and (E) intact chili pepper with pedicel. Sub-panels (1, 2, and 3) correspond to the LG, IC, and FR maturity stages, respectively.

To understand the physiological behavior of the samples during storage, changes in O_2 and CO_2 concentrations were monitored across different anatomical parts and maturity stages of chili pepper (Fig. 3). Distinct gas profiles were observed among the anatomical fractions. The pedicel (A1–A3) showed relatively small changes in gas composition, with O_2 remaining comparatively high and only a limited increase in CO_2 throughout storage, indicating relatively low respiratory activity. In contrast, the seeds (B1–B3), pericarp (C1–C3), intact chili pepper without pedicel (D1–D3), and intact chili pepper with pedicel (E1–E3) exhibited a progressive decline in O_2 accompanied by CO_2 accumulation. These changes became more pronounced with advancing maturity, particularly at the FR stage, where O_2 depletion and CO_2 accumulation occurred more rapidly than at the LG and IC stages. The most substantial changes were observed in the pericarp, especially at the IC and FR stages (C2–C3), where O_2 rapidly decreased to very low concentrations while CO_2 increased to approximately 20%, indicating intensive respiratory activity and restricted gas exchange within the tissue. Similar, although less pronounced, patterns were observed in intact fruits (D2–D3 and E2–E3), suggesting that the structural resistance of the fruit may limit gas diffusion between internal tissues and the surrounding atmosphere (Nugraha *et al*., 2022).

These gas concentration profiles were further quantified using the respiration kinetic parameters presented in Table 1. The respiration rates ranged from 0.03 to 0.19 mL g^{-1} h^{-1}, showing a higher magnitude compared with whole-fruit measurements reported in previous studies (Lon Kan *et al*., 2019), which may be associated with differences in anatomical isolation and respiration-tracking methods. Among the anatomical fractions, the highest reference O_2 consumption rate (V_{m,O_2}) was observed in the seeds, reflecting their substantial metabolic contribution despite the general decline in respiration during ripening (Xiao *et al*., 2018). Furthermore, the interaction between O_2 availability and CO_2 accumulation was characterized by the Michaelis–Menten constants. K_{mO2} represents the O_2 concentration at which the respiration rate reaches half of its maximum value, whereas K_{mCO2} represents the CO_2 concentration causing 50% inhibition of O_2 consumption (Castellanos *et al*., 2017). As shown in Table 1, these kinetic constants varied among anatomical parts and maturity stages, further demonstrating that respiratory behavior is strongly influenced by both tissue characteristics and fruit maturity.

Table 1. Non-linear regression analysis for O_2 uptake by the anatomy parts of the chili pepper for a non-competitive inhibitor

Anatomy part of chili	Non-competitive inhibitor				
	$V_{m,O2}$	K_{mO2}	K_{mnCO2}	RW. ox	R^2
Large Green (LG)					
Intact chili	0.06	2.443	4.02	0.53	0.99
Without pedicel	0.07	2.39	3.98	0.63	0.71
Pericarp	0.09	4.38	2.76	0.03	0.90
Seed	0.03	1.79	3.49	0.62	0.82
Pedicel	0.03	0.00	1.50	0.00	0.83
Initial Coloring (IC)					
Intact chili	0.05	13.86	7.37	0.53	0.86
Without pedicel	0.04	3.21	5.66	0.63	0.66
Pericarp	0.09	3.88	5.10	0.03	0.99
Seed	0.06	0.03	0.01	0.62	0.93
Pedicel	0.05	0.10	1.70	0.00	0.83
Full Red (FR)					
Intact chili	0.06	1.44	2.35	0.27	0.80
Without pedicel	0.05	1.51	3.92	0.37	0.90
Pericarp	0.11	0.75	2.24	0.18	0.87
Seed	0.09	0.08	4.93	0.08	0.93
Pedicel	0.09	0.00	1.99	0.00	0.61

3.2. Respiration rate of the chili pepper anatomical parts

Fig. 4 presents the respiration rates of the whole fruit and its anatomical fractions at three maturity stages. Respiration was highest at the large green (LG) stage in all parts, declined at the initial coloring (IC) stage, and reached its lowest values at the full red (FR) stage as the fruit approached senescence. Among the fractions, seeds and pedicels showed

the highest rates, particularly at the LG stage (0.055 ± 0.009 and 0.064 ± 0.006 mL·g^{-1}·h^{-1}, respectively). Seed respiration can be several times higher than that of the whole fruit (Xiao *et al*., 2018), where it was elevated at LG, moderate at IC, and negligible at FR, consistent with peak seed mass during early fruit development (Rolletschek *et al*., 2025) and with the measured seed weights of 0.503 ± 0.067, 0.279 ± 0.031, and 0.297 ± 0.035 g at the LG, IC, and FR stages, respectively.

The elevated respiration of the pedicel at the LG and IC stages is attributed to its higher permeability relative to the pericarp (O'Donoghue *et al*., 2018) and its role as an O_2 diffusion pathway through cuticular structures (Xiao *et al*., 2018). Notably, intact fruit without the pedicel respired more than intact fruit with the pedicel at all maturity stages, despite the pedicel itself having the highest rate of any fraction. This apparent contradiction indicates that pedicel removal induces wound respiration at the detachment site, which outweighs the loss of the pedicel's own respiratory contribution and accelerates tissue deterioration (Alhassan *et al*., 2019).

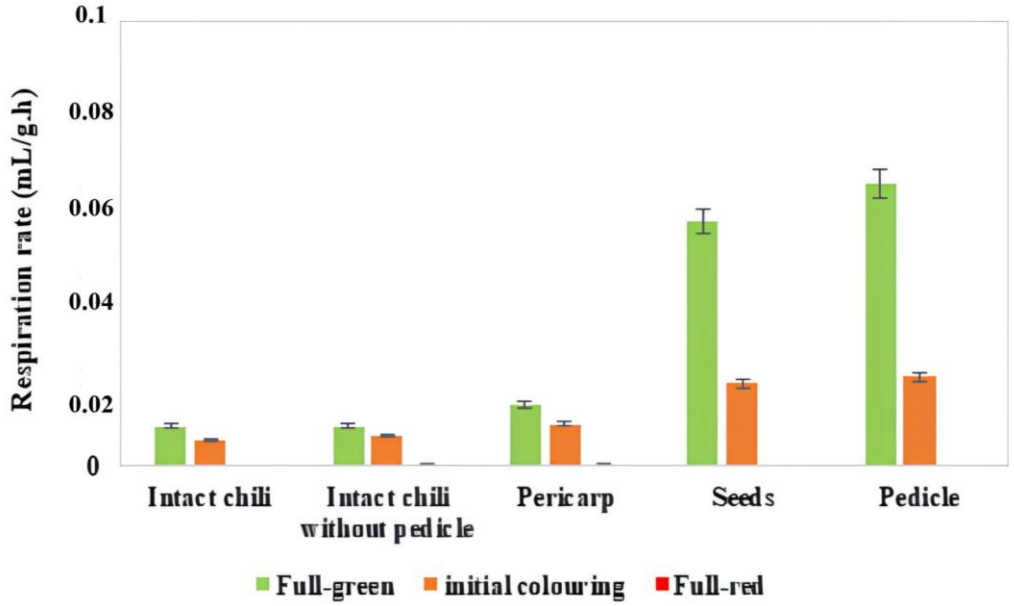


Figure 4. Respiration rate (25 °C) for various ripening stages (full-green, initial colouring, and full-red) with various anatomical parts (intact chili pepper, intact chili pepper without pedicel, pericarp, seeds, and pedicel). Data are means + SE, n = 10 (two-way ANOVA, $p < 0.05$)

3.3. Three-Dimensional Internal Architecture of Chili Pepper

Using CT, the internal air space of chili pepper fruit was quantified at a volume of 0.264 ± 0.033 cm^3, constituting approximately 13% of the total volume (1.904 ± 0.021 cm^3). On the other hand, this air space volume was remarkably similar to the volume of the placenta (0.262 ± 0.041 cm^3), as shown in Figure 5. While an increase in internal air space is often a characteristic of post-harvest weight loss (Li *et al*., 2024), these internal cavities played a crucial role as reservoirs for gas exchange. However, the structural analysis revealed that these air spaces were not directly connected to the pedicel, which aligns with post-harvest morphological phenomena previously reported by Xiao *et al*. (2018). Because the internal air spaces were structurally isolated from the pedicel, gas transport into the inner organs must have relied on a different pathway. 3D visualization highlighted the placenta as the primary structural bridge connecting the internal seeds to the external pedicel (Figure 5A and 5C). Hence, the visualization confirmed the pedicel lenticels as the primary gateway for O_2 uptake and CO_2 production.

This specific anatomical arrangement explained the respiratory dynamics and the COL of the chili pepper. Because gas must diffuse through the dense placental tissue to reach the seeds, a significant internal diffusion resistance was generated. This structural bottleneck restricts O_2 availability in the internal organs, explaining why the seeds and

pedicel exhibit different respiration behaviors compared to the pericarp. Consequently, this internal resistance dictates the high COL of the intact fruit. If the external O_2 concentration drops near the COL during storage of MAP, the restricted diffusion pathway will cause the localized O_2 at the placenta and seeds to deplete even further, immediately triggering anaerobic respiration, ethanol production, and ultimately internal cell death (Xiao *et al*., 2018).

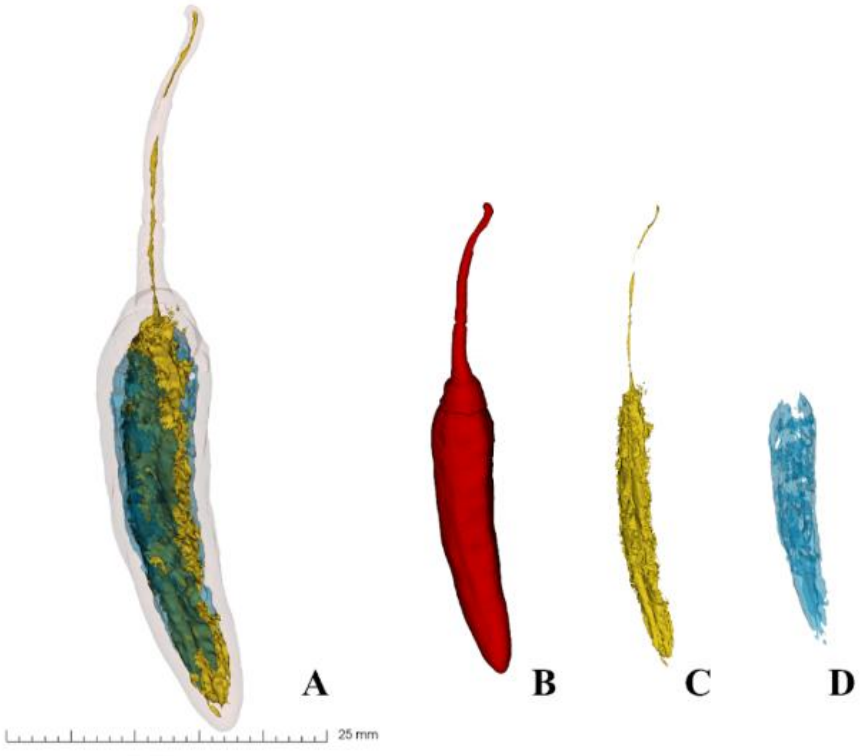


Figure 5. (A) The three-dimensional segmented internal architecture of chili pepper consisted of (B) macro-structure, (C) placenta tissue, and (D) air space

3.4. Critical Oxygen Level

The critical oxygen limit acts as an indicator of the lowest tolerance limit for oxygen in the environment (Nugraha *et al*., 2022). As shown in Figure 6, the COL across all anatomical parts and ripeness levels of chili pepper is in the very low range of 0% to 0.629%. The lowest COL values were consistently observed in separately measured internal organs, namely the seeds and pedicels, across all ripeness levels. The low COL in isolated seeds indicates their capacity to maintain respiration under low-oxygen conditions, primarily because measuring them separately removes the structural resistance and intercellular gas gradients normally imposed by the pericarp (Rolletschek *et al*., 2025) Similarly, the isolated pedicel exhibited a low COL due to its abundance of gas-exchange facilitators (lenticels) and sclerenchyma/xylem tissue, which have lower metabolic activity compared to the pericarp (O'Donoghue *et al*., 2018).

In contrast, the highest COL was observed in LG fruit from which the pedicel had been removed (0.629%), a value significantly greater than that of all other combinations of anatomical part and ripeness level (Tukey's HSD, $p < 0.05$) (Figure 6). These results indicate that LG intact fruits are highly susceptible to hypoxia under very low oxygen conditions, driven by a combination of high internal diffusion resistance and increased metabolic activity during this early development stage (Nugraha *et al*., 2022; Boeckx *et al*., 2019). Conversely, fruits at the IC stage demonstrated a much higher tolerance to low oxygen, with COL values dropping to near-zero (0.019% and 0.012%). However, as the fruit reached the FR, the COL for intact chili peppers increased again to approximately 0.211%. Consequently, managing these respiration dynamics and oxygen thresholds during commercial handling is vital for maintaining postharvest quality and extending shelf life in the storage environment (Gross *et al*., 2016).

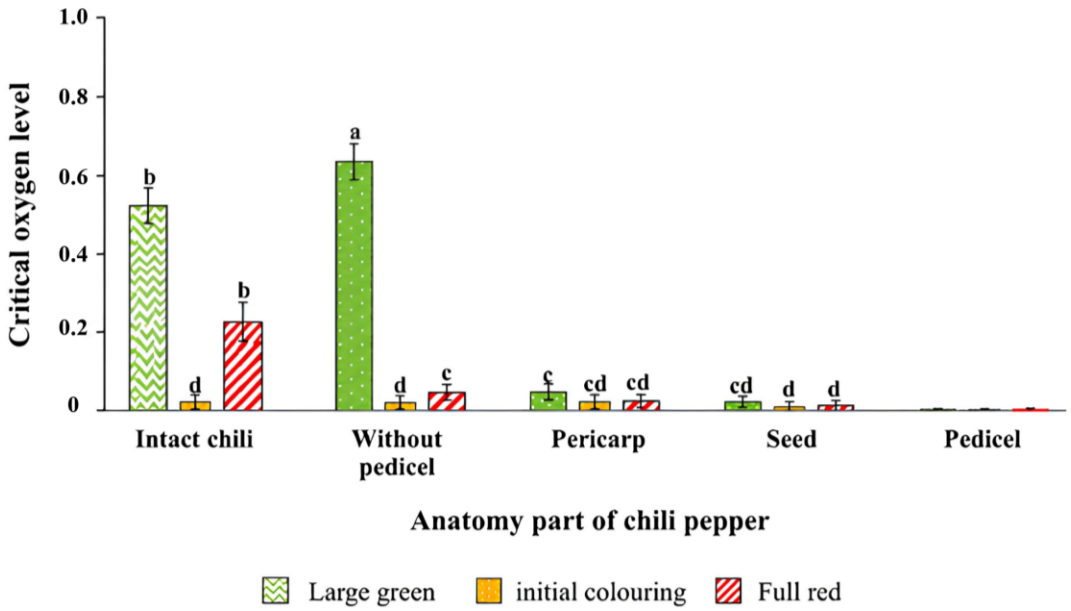


Figure 6. Limit oxygen level in various anatomical parts of the chili pepper fruit at three different levels of ripeness

3.5. Respiratory Quotient

The critical O_2 limit (C^*O_2) is the lowest O_2 concentration a chili pepper can tolerate before CO_2 production exceeds what aerobic respiration can support. The corresponding RQ limit (RQ*) was calculated by substituting C^*O_2 into the respiration model (Eq. 5), neglecting the minor inhibitory effect of CO_2 (Nugraha *et al*., 2022). Because RQ* marks the point at which fermentative metabolism begins to dominate, it provides a tissue-specific threshold for defining safe storage atmospheres.

Figure 7 shows the RQ limits across chili pepper anatomical parts and maturity stages. Seeds and pedicels had lower RQ values than the intact fruit and pericarp, with the lowest values at the FR stage, reflecting limited respiratory activity and a minimal contribution to anaerobic metabolism (Xiao *et al*., 2018). The intact fruit and pericarp, by contrast, showed higher RQ values that generally increased with maturity; intact fruit with and without the pedicel reached approximately 1.2–1.35 at the IC and FR stages, indicating a greater tendency toward CO_2 evolution relative to O_2 consumption under those conditions. The pericarp maintained a consistently high RQ limit across all maturity stages, reflecting its substantial contribution to CO_2 evolution under diffusion-restricted conditions (Xiao *et al*., 2021). These distinct variations across fractions show that whole-fruit measurements do not fully reflect the metabolic behavior of the internal tissues (Iglesias-Sanchez *et al*., 2026), an important consideration for modified atmosphere packaging design, since RQ values exceeding tissue-specific thresholds can trigger anaerobic metabolism and compromise fruit quality.

The observed increase in the RQ limit with maturity in intact fruit indicates greater susceptibility to anaerobic metabolism at the full red stage. Decreased gas diffusivity and changes in respiratory pathways in ripening fruit lead to increased CO_2 production relative to O_2 (Xiao *et al*., 2021). Such changes in respiratory metabolism may influence tolerance to low-oxygen storage environments. The pericarp exhibited a consistently high RQ limit across all stages of maturity, indicating that pericarp tissue has a higher propensity to shift towards fermentative pathways when oxygen becomes limited. This is likely because the pericarp contributes substantially to CO_2 evolution under hypoxic conditions (Li & Terzoudis, 2024). The pericarp exhibited a high RQ limit across all maturity stages. This is attributed to its dominant volume and restricted gas diffusion, where the spatial architecture of the internal air spaces (as visualized in Figure 5) imposes physical barriers that limit optimal aerobic respiration (Xiao *et al*., 2021).

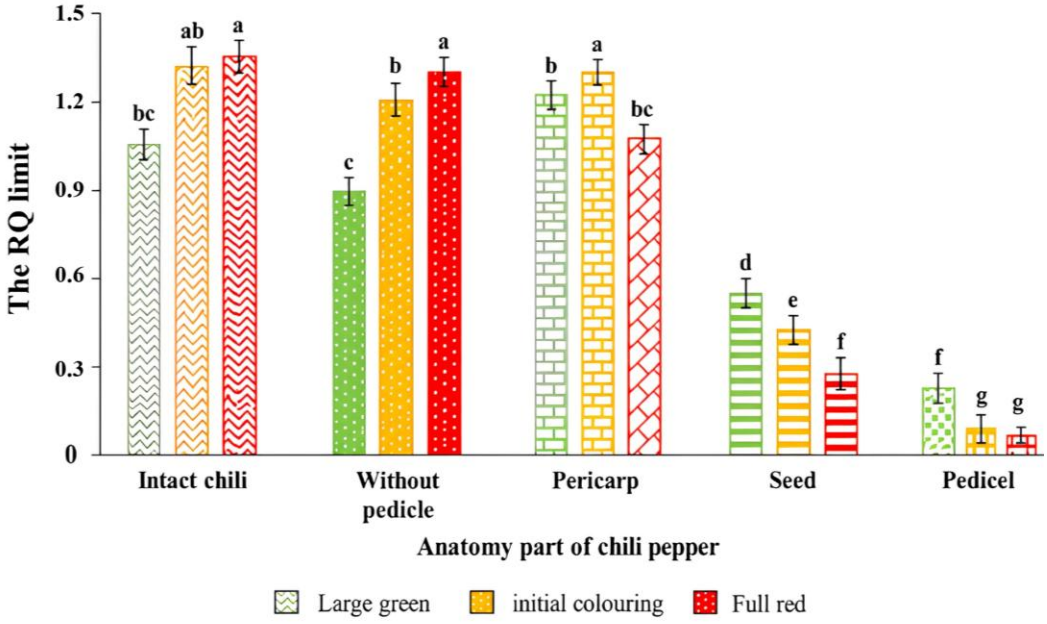


Figure 7. Respiratory quotient (RQox) values in various anatomical

4. CONCLUSIONS

Respiration characteristics and critical oxygen limit of chili peppers vary significantly across maturity stages and anatomical fractions. The LG stage exhibits the highest respiration rates, with isolated seeds and pedicels showing elevated metabolic activities (0.055 ± 0.009 and 0.064 ± 0.006 $mL.g^{-1}.h^{-1}$, respectively). Furthermore, COL spans from 0% to 0.629%, where LG intact fruits and isolated internal organs display superior tolerance to low-oxygen environments. These distinct anatomical and developmental variations demonstrate that intact chili measurements do not fully reflect tissue-specific traits, providing a precise physiological foundation for optimizing MAP and cold storage conditions.

ACKNOWLEDGMENTS

This work was supported by the Laboratory of Food and Postharvest Engineering, the Computer-aided Postharvest Technology (CaPT) of the Faculty of Agricultural Technology, Universitas Gadjah Mada, and by the Indonesia Endowment Fund for Education (LPDP) (Grant Number: 202401110300300).

AUTHOR CONTRIBUTION

Author	C	M	So	Va	Fo	I	R	D	O	E	Vi	Su	P	Fu
HS	✓	✓	✓	✓	✓	✓	✓	✓	✓	✓	✓		✓	✓
MA		✓		✓	✓	✓	✓		✓	✓				
YAF		✓	✓	✓	✓	✓	✓	✓	✓	✓	✓			✓
SR			✓	✓	✓	✓	✓	✓		✓	✓	✓		✓
BN	✓	✓	✓	✓	✓	✓	✓	✓	✓	✓	✓	✓	✓	✓

C: Conceptualization	Fo: Formal Analysis	O: Writing - Original Draft	Fu: Funding Acquisition
M: Methodology	I: Investigation	E: Writing - Review & Editing	P: Project Administration
So: Software	D: Data Curation	Vi: Visualization	
Va: Validation	R: Resources	Su: Supervision	

DECLARATION OF GENERATIVE AI UTILIZATION

Not applicable. The authors did not use any generative AI tools or services in the preparation of this manuscript. All content is entirely the intellectual work of the authors.

REFERENCES

Alhassan, N., Golding, J.B., Wills, R.B.H., Bowyer, M.C., & Pristijono, P. (2019). Long term exposure to low ethylene and storage temperatures delays calyx senescence and maintains "afourer" mandarins and navel oranges quality. *Foods*, ***8***(1). https://doi.org/10.3390/foods8010019

Benkeblia, N. (2021). Physiological and Biochemical Response of Tropical Fruits to Hypoxia/Anoxia. In *Frontiers in Plant Science* (Vol. 12). https://doi.org/10.3389/fpls.2021.670803

Brizzolara, S. (2020). Primary Metabolism in Fresh Fruits During Storage. In *Frontiers in Plant Science* (Vol. 11). https://doi.org/10.3389/fpls.2020.00080

Castellanos, D.A., Mendoza, R., Gavara, R., & Herrera, A.O. (2017). Respiration and ethylene generation modeling of "Hass" avocado and feijoa fruits and application in modified atmosphere packaging. *International Journal of Food Properties*, ***20***(2), 333–349. https://doi.org/10.1080/10942912.2016.1160921

Chitravathi, K., Chauhan, O.P., & Raju, P.S. (2015). Influence of modified atmosphere packaging on shelf-life of green chillies (*Capsicum annuum* L.). *Food Packaging and Shelf Life*, ***4***, 1–9. https://doi.org/10.1016/j.fpsl.2015.02.001

Del Giúdice, L.Z., Falquetto-Gomes, P., de Almeida Costa, P.M., Martins, A.O., Omena-Garcia, R.P., Araújo, W.L., Zsögön, A., Picoli, E.A. de T., & Nunes-Nesi, A. (2023). Dynamic shifts in primary metabolism across fruit development stages in Capsicum chinense (cv. Habanero). *Journal of Plant Physiology*, ***291***(May). https://doi.org/10.1016/j.jplph.2023.154121

Du, Z., Hu, Y., Ali Buttar, N., & Mahmood, A. (2019). X-ray computed tomography for quality inspection of agricultural products: A review. *Food Science and Nutrition*, ***7***(10), 3146–3160. https://doi.org/10.1002/fsn3.1179

Garavito, J., Herrera, A.O., & Castellanos, D.A. (2021). A combined mathematical model to represent transpiration, respiration, and water activity changes in fresh cape gooseberry (Physalis peruviana) fruits. *Biosystems Engineering*, ***208***, 152–163. https://doi.org/10.1016/j.biosystemseng.2021.05.015

Gross, K.C., Wang, C.Y., & Saltveit, M.E. (eds). (2016). The commercial storage of Fruits, Vegetables, and Florist and Nursery Stocks. *Agricultural Research Service, United States Department of Agriculture, Wahington DC*, ***66***(66), 442. www.ntis.gov.

Han, S.H., Jang, H.D., & Lee, S.J. (2020). Modeling respiration rates of Ipomoea batatas (sweet potato) under hermetic storage system. *Food Science and Biotechnology*, ***29***(2), 227–234. https://doi.org/10.1007/s10068-019-00660-2

Ho, P.L., Tran, D.T., Hertog, M.L.A.T.M., & Nicolaï, B.M. (2020). Modelling respiration rate of dragon fruit as a function of gas composition and temperature. *Scientia Horticulturae*, ***263***(October 2019), 109138. https://doi.org/10.1016/j.scienta.2019.109138

Hou, B.Z., Li, C.L., Han, Y.Y., & Shen, Y.Y. (2018). Characterization of the hot pepper (*Capsicum frutescens*) fruit ripening regulated by ethylene and ABA. *BMC Plant Biology*, ***18***(1), 1–12. https://doi.org/10.1186/s12870-018-1377-3

Iglesias-Sanchez, A., García-Carbonell, S., Fernie, A.R., Pujol, M., & Florez-Sarasa, I. (2026). Fruit respiration: putting alternative pathways into perspective. *New Phytologist*, ***250***(1), 54–73. https://doi.org/10.1111/nph.70882

Lestari, E.P., Prajanti, S.D.W., Wibawanto, W., & Adzim, F. (2022). ARCH-GARCH Analysis: An Approach to Determine The Price Volatility of Red Chili. *Agraris*, ***8***(1), 90–105. https://doi.org/10.18196/agraris.v8i1.12060

Li, X., Shen, D., Mao, J., Zhang, L., Mao, J., Chen, B., & Bi, Y. (2024). Increased weight loss and internal air space, degraded starch and pectin combined to cause pulp mealiness in 'Oregon Spur II' apples during ambient storage. *Scientia Horticulturae*, ***324***(November 2023), 112629. https://doi.org/10.1016/j.scienta.2023.112629

Li, X, & Terzoudis, K. (2024). Tissue-specific responses of the central carbon metabolism in tomato fruit to low oxygen stress.

Lon Kan, E.E., Sargent, S.A., Cantliffe, D.J., Berry, A.D., & Shaw, N.L. (2019). Harvest maturity and storage temperature affect postharvest quality of 'wanda' datil hot pepper grown under protected culture. *HortTechnology*, ***29***(4), 402–407. https://doi.org/10.21273/HORTTECH04328-19

Mahajan, P.V., Caleb, O.J., Gil, M.I., Izumi, H., Colelli, G., Watkins, C.B., & Zude, M. (2017). Quality and safety of fresh

horticultural commodities: Recent advances and future perspectives. *Food Packaging and Shelf Life*, ***14***(July), 2–11. https://doi.org/10.1016/j.fpsl.2017.08.001

Malakar, S., Kumar, N., Sarkar, S., & Mohan, R.J. (2020). Influence of Modified Atmosphere Packaging on the Shelf Life and Postharvest Quality Attributes of King Chili (Capsicum chinense Jacq.) during Storage. *Journal of Biosystems Engineering*, ***45***(4), 213–222. https://doi.org/10.1007/s42853-020-00057-8

Munarso, S.J., Kailaku, S.I., bin Arif, A., Budiyanto, A., Mulyawanti, I., Sasmitaloka, K.S., Setyawan, N., Dewandari, K.T., & Widayanti, S.M. (2020). Quality analysis of chili treated with aqueous ozone treatment and improved transportation and handling technology. *International Journal of Technology*, ***11***(1), 37–47. https://doi.org/10.14716/ijtech.v11i1.3213

Nugraha, B., Verboven, P., Verlinden, B.E., Verreydt, C., Boone, M., Josipovic, I., & Nicolaï, B.M. (2022). Gas exchange model using heterogeneous diffusivity to study internal browning in 'Conference' pear. *Postharvest Biology and Technology*, ***191***(June). https://doi.org/10.1016/j.postharvbio.2022.111985

O'Donoghue, E.M., Brummell, D.A., McKenzie, M.J., Hunter, D.A., & Lill, R.E. (2018). Sweet capsicum: postharvest physiology and technologies. *New Zealand Journal of Crop and Horticultural Science*, ***46***(4), 269–297. https://doi.org/10.1080/01140671.2017.1395349

Pathare, P.B., Al-Dairi, M., Al-Yahyai, R., & Al-Mahdouri, A. (2023). Physiological Response of Stored Pomegranate Fruit Affected by Simulated Impact. *Foods*, ***12***(6). https://doi.org/10.3390/foods12061122

Rolletschek, H., Borisjuk, L., Gómez-Álvarez, E.M., & Pucciariello, C. (2025). Advances in seed hypoxia research. *Plant Physiology*, ***197***(1), 1–13. https://doi.org/10.1093/plphys/kiae556

Surya, R., & Tedjakusuma, F. (2022). Diversity of sambals, traditional Indonesian chili pastes. *Journal of Ethnic Foods*, ***9***(1). https://doi.org/10.1186/s42779-022-00142-7

Triardianto, D., Subaktillah, Y., Sirojul Anam Izza Rosyadi, A., Choirun, A., & Widyaningtyas, S. (2026). Respiration rate modeling of Cavendish banana (*Musa acuminata* cv. Cavendish) under various storage temperatures. *BIO Web of Conferences*, ***210***, 1–10. https://doi.org/10.1051/bioconf/202621002010

Webb, A.J., & Kosasih, I.A. (2016). Analysis of Price Volatility in the Indonesia Fresh Chili Market. *Annual Meeting of the International Agricultural Trade Research Consortium*, 1–10.

Xiao, H., Piovesan, A., Pols, S., Verboven, P., Nicolai, B. (2021). Microstructural changes enhance oxygen transport in tomato (Solanum lycopersicum) fruit during maturation and ripening. *New Phytologist*, ***232***(5), 2043–2056. https://doi.org/10.1111/nph.17712

Xiao, Z., Rogiers, S.Y., Sadras, V.O., Tyerman, S.D. (2018). Hypoxia in grape berries: The role of seed respiration and lenticels on the berry pedicel and the possible link to cell death. *Journal of Experimental Botany*, ***69***(8), 2071–2083. https://doi.org/10.1093/jxb/ery039